ARTICLE

Catalytic Transformation of Bio-oil to Olefins with Molecular Sieve Catalysts

Wei-wei Huang, Fei-yan Gong, Qi Zhai, Quan-xin Li*

Department of Chemical Physics, University of Science and Technology of China, Hefei 230026, China

(Dated: Received on April 23, 2012; Accepted on May 22, 2012)

Catalytic conversion of bio-oil into light olefins was performed by a series of molecular sieve catalysts, including HZSM-5, MCM-41, SAPO-34 and Y-zeolite. Based on the light olefins yield and its carbon selectivity, the production of light olefins decreased in the following order: HZSM-5>SAPO-34>MCM-41>Y-zeolite. The highest olefins yield from bio-oil using HZSM-5 catalyst reached 0.22 $kg/kg_{bio\text{-}oil}$ with carbon selectivity of 50.7% and a nearly complete bio-oil conversion. The reaction conditions and catalyst characterization were investigated in detail to reveal the relationship between the catalyst structure and the production of olefins. The comparison between the pyrolysis and catalytic pyrolysis of bio-oil was also performed.

Key words: Bio-oil, Olefins, Catalytic pyrolysis, Molecular sieve catalyst

I. INTRODUCTION

Light olefins (*i.e.*, ethylene, propylene and butylenes), which are the basic feedstocks for the petrochemical industry, are primarily produced through steam cracking and fluid catalytic cracking (FCC) using naphtha, light diesel and other petroleum products as feedstocks at present [1, 2]. Biomass, a rich, environmentally friendly and renewable resource, can be used as an alternative feedstock for the production of biofuels and biochemicals [3]. In principle, biomass can be firstly converted to syngas through the biomass gasification or bio-oil reforming process, followed by the catalytic conversion of biomass-derived syngas to light olefins [3]. However, this route may be limited by the Anderson-Schulz-Flory (ASF) distribution as well as high-pressure operation [4, 5].

Bio-oil, produced from fast pyrolysis of various plant components of lignocellulosic biomass, has been identified as a renewable feedstock for the production of renewable fuels and commodity chemicals [6−9]. The catalytic cracking of bio-oil is another route of the production of olefins from biomass. Compared with solid biomass as the raw material, liquid bio-oil, which can be readily stored and transported, is more suitable for the production of chemicals on a large scale. Production of olefins from the catalytic cracking of bio-oil may be unrestricted by the ASF distribution. As compared with the common feedstocks such as naphtha and light diesel used for the production of light olefins, bio-oil possesses some unique composition characters, such as higher content of oxygen. Also, the complex reactions are generally involved in the bio-oil catalytic transformation process due to the composition complexity of bio-oil. The yield of light olefins from bio-oil is mainly determined by the ability of a catalyst to selectively cracking the oxygenated organic compounds in bio-oil. When the oxygen in the bio-oil is removed as CO and CO_2, the production of light olefins from the oxygenated organic compounds in bio-oil (represented by $C_xH_yO_z$) can be briefly described by the following overall expressions:

$$C_xH_yO_z \rightarrow C_nH_{2n}\ (n{=}2-4) + CO + H_2O \quad (1)$$

$$C_xH_yO_z \rightarrow C_nH_{2n}\ (n{=}2-4) + CO_2 + H_2O \quad (2)$$

Up to now, there is rarely reported literature about production of light olefins from bio-oil, and the catalytic cracking of the bio-oil model compounds such as ethanol, butanol, phenols, acetone, acetic acid over the HZSM-5 zeolite catalyst were mainly focused on [10−13]. Both the selectivity and yield of light olefins derived from bio-oil are noticeably lower than those from methanol, ethanol and naphtha, thereby it is needed to improve them by optimizing the catalysts and cracking conditions. The main challenge in the catalytic conversion of biomass derived feedstocks is how to improve catalyst and process conditions to obtain high yields of target products [14]. Zeolite catalysts, which are widely used in the petroleum industry [15, 16], may be promising for conversion of biomass derived feedstocks into fuels and chemicals [17−20].

In this work, the production of light olefins through a series of molecular sieve catalysts, including HZSM-5, MCM-41, SAPO-34, and Y-zeolite are investigated. The types of molecular sieve catalysts and reaction conditions have an important impact both on olefins yield and its selectivity. The conversion of bio-oil to light olefins may potentially provide a useful approach to

*Author to whom correspondence should be addressed. E-mail: liqx@ustc.edu.cn

producing the key building blocks in the petrochemical industry from the renewable biomass.

II. EXPERIMENTS

A. Feedstock

Bio-oil was produced by the fast pyrolysis of biomass in a circulating fluidized bed with a oil capacity of 120 kg/h at our lab [21−25]. The main elemental composition of bio-oil feedstock derived from fast pyrolysis of straw stalk is 42.3%C, 7.9%H, and 49.4%O. Water content in the bio-oil is about 24.4%. The chemical formula of the oxygenated organic compounds of the bio-oil feed can be expressed as $CH_{2.12}O_{0.89}$.

B. Catalyst preparation and characterization

The HZSM-5 zeolite with Si/Al ratio of 25 was prepared by the following procedure [26]. The sodium form zeolite was first converted to the H form via $NH_4{}^+$ exchange procedure, followed by calcinating at 550 °C. The impregnation method was adopted to load magnesium into the HZSM-5 zeolite. The HZSM-5 zeolite was impregnated in the solution of magnesium nitrate for a night, followed by rotary-evaporation at 60 °C, drying at 80 °C for 6 h, and calcinating at 550 °C for 5 h. Other catalysts used, including MCM-41, SAPO-34, and Y-zeolite, were purchased from Nankai university catalyst Co., Ltd. in China.

The prepared catalysts were investigated by the NH_3-temperature rogrammed desorption of ammonia (TPD), X-ray diffraction (XRD), ^{29}Si MAS NMR (magic angle spin nuclear magnetic resonance), and TGA (Thermogravimetric analyses) analyses. For the NH_3-TPD tests, the catalyst was firstly pretreated at 500 °C in a helium flow (ultrahigh purity, 100 mL/min) for 2 h, and then adsorption of ammonia was carried out at 120 °C for 1 h. After the catalyst was flushed with He at 120 °C for 1 h, the programmed-desorption of NH_3 was run from 120 °C to 700 °C with a heating rate of 10 °C/min. The amount of desorbed ammonia was measured by a gas chromatograph (GC-SP 6890) with a thermal conductivity detector (TCD) detector. XRD patterns of the catalysts were recorded on an X'pert Pro Philips diffractrometer, using a Cu Kα radiation (λ=0.15418 nm). The ^{29}Si MAS NMR spectra was scanned using a Bruker AVANCE AV400 (Bruker BioSpin GmbH) spectrometer, where the ^{29}Si chemical shifts were referenced to tetramethylsilane (TMS) at 0 ppm. TGA were carried out with a Q5000 TGA system (TA Instruments). The sample temperature was programmed from room temperature to 1000 °C at a rate of 10 °C/min.

C. Experimental setup and product analysis

The production of light olefins from the catalytic cracking of bio-oil was carried out in the continuous-flowing systems, using a quartz fixed-bed reactor under atmospheric pressure. This system consists of a quartz tube reactor (inner diameter: 30 mm, length: 400 mm), a gas feed system, a liquid feeding pump, a heater and temperature control system, a condenser and an on-line gas analysis unit, which has been described in detail previously [21−25]. Sieved zeolite catalyst powders (60−80 mesh) were held in the reactor by quartz beads. The liquid reactants were fed into the reactor using a multisyringe pump (TS2-60, Baoding Longer Precision Pump). The steam from a steam generator, which was controlled by the mass flow controller, was used as carrier gas. Before reaction, the reactor was flushed by argon with the flow rate of 30 sccm for 1 h at the room temperature, and then was externally heated to a given temperature by the carborundum heaters with a programmed temperature controller.

The gaseous products were analyzed using an on-line GC equipped with two detectors, a TCD for analysis of H_2, CO, CH_4 and CO_2 separated on TDX-01 column, and a flame ionization detector (FID) for gaseous hydrocarbons separated on a Porapak-Q column. The liquid products obtained in each experiment were weighed to calculate their yields, and subsequently stored in sealed glass jars for further analysis. The liquid products were analyzed using a GC (SP 6890) with a FID detector and a SE30 capillary column, and further confirmed by a GC-MS (Thermo Trace DSQ (I)) with a TR-5MS fused-silica capillary column. The coke deposited on the catalyst has been studied by combustion with air in the TG/MS arrangement. The performance of production of light olefins via the catalytic cracking of bio-oil was evaluated by the bio-oil conversion ($C_{\text{conv.}}$), absolute light olefins yield (Y_{olefins}), light olefins distribution (D_n) and the products selectivity of (S_{X}) according to the following equations:

$$C_{\text{conv.}} = \frac{x_{\text{inC}}}{X_{\text{inC}}} \times 100\% \tag{3}$$

$$Y_{\text{olefins}} = \frac{y_{\text{olefins}}}{y_{\text{feed}}} \times 100\% \tag{4}$$

$$D_n = \frac{x_{\text{C}_n\text{H}_{2n}}}{x_{\text{olefins}}} \times 100\% \tag{5}$$

$$S_{\text{X}} = \frac{x_{\text{X}}}{X_{\text{inC}}} \times 100\% \tag{6}$$

where x_{inC} and X_{inC} are moles of C in all identified products and C feed in, respectively; y_{olefins} and y_{feed} are mass of light olefins and feed, respectively; $x_{\text{C}_n\text{H}_{2n}}$ and x_{olefins} are moles of C in C_nH_{2n} and all light olefins; and x_{X} is moles of C in X, X represents light olefins, CO, CO_2, CH_4, C2−C4 alkanes or C5$^+$ hydrocarbons.

All the tests were repeated three times. The difference for each replicate generally is less than 10 % and the mass balance of the fed biomass is over 90 %. The

DOI:10.1088/1674-0068/25/04/441-447

TABLE I Performance of the catalytic cracking of bio-oil over different types of molecular sieve catalysts. Reaction conditions: T=600 °C, S/C=10, WHSV=0.4 h^{-1}.

Catalysts	C/%	$Y_{olefins}$/(kg/$kg_{bio-oil}$)	S_X/%						D_n/%		
			$C2^=-C4^=$	CO	CO_2	CH_4	C2−C4	$C5^+$	C_2H_4	C_3H_6	C_4H_8
HZSM-5	90.2	0.22	50.7	16.2	14.8	4.1	2.9	11.3	48.6	44.3	7.1
MCM-41	63.4	0.11	20.8	14.4	13.8	8.9	4.0	38.1	37.2	32.6	30.2
SAPO-34	72.2	0.17	34.4	17.5	10.5	4.2	3.5	29.9	39.4	24.4	36.2
Y-zeolite	70.6	0.06	14.2	31.5	5.8	16.2	2.3	30.0	48.0	44.2	7.8

reported data are the mean values of three trials.

III. RESULTS AND DISCUSSION

A. Performance of different types of molecular sieve catalysts

Table I presents the performance of the production of light olefins from bio-oil with different types of molecular sieve catalysts, including HZSM-5, MCM-41, SAPO-34 and Y-zeolite, under the typical catalytic cracking conditions of T=600 °C, S/C (the molar ratio of steam to carbon fed)=10 and WHSV (the mass flow rate of the feed divided by the mass of the catalyst)=0.4 h^{-1}. The main products observed contain $C2^=-C4^=$ light olefins, CO, CO_2, CH_4, $C5^+$ hydrocarbons (including aromatics, $C5^+$ alkanes and olefins) and C2−C4 alkanes for all tested catalysts. However, it was found that the performance of the production of light olefins from bio-oil was quite different over different types of molecular sieve catalysts, which should be related to their different structures and varied pore sizes of the zeolite catalysts. Based on the light olefins yield and its carbon selectivity, the production of light olefins decreases in the following order: HZSM-5>SAPO-34>MCM-41>Y-zeolite. Especially, the HZSM-5 catalyst has a 3-dimensional regular pore system with the pore size of 5.5−5.6 Å. The smaller pore size and internal volume make it difficult for larger $C5^+$ hydrocarbons to form inside of the pores. The bio-oil conversion over HZSM-5 was about 90% at 600 °C. The total yield of $C2^=-C4^=$ light olefins was about 0.22 $kg_{olefins}/kg_{bio-oil}$ with a carbon selectivity of light olefins of 50.7%. Thus, we pay more attention to the production of light olefins from bio-oil with the HZSM-5 catalyst.

B. Effect of reaction temperature

Figure 1 shows the effect of temperature on the production of light olefins from the bio-oil over the HZSM-5 catalyst under the following conditions: T=450−750 °C, S/C=10 and WHSV=0.4 h^{-1}. The total bio-oil conversion increased from 65.9% to 94.0% with increasing temperature from 450 °C to 650 °C, and was close to an complete conversion at 750 °C. High temperature is more favorable to the catalytic cracking of the bio-oil. The carbon selectivity of the main products decreases in the following order at 600 °C: $C2^=-C4^=$ light olefins>CO>CO_2>$C5^+$ hydrocarbons>CH_4>C2−C4 alkanes. The light olefins selectivity goes through a maximum of 50.7% near 600 °C. Further increasing temperature to 750 °C significantly reduced the olefins selectivity to 35.6%. The CO and CH_4 selectivity increased with increasing temperature. But the $C5^+$ hydrocarbons selectivity decreased with temperature. This result indicates that the high temperature favors to decompose heavier molecules to smaller molecules through pyrolysis and catalytic pyrolysis. Also, the secondary reactions of the intermediate oxygenates should further enhance, leading to an increase in the small molecular gas products. The total yield of $C2^=-C4^=$ light olefins presents a maximum value around 600 °C. The rapid reduction in the olefins yield over 600 °C is mainly owing to the increase in the CO and CH_4 selectivity and the decrease in the olefins selectivity. An exorbitant temperature will also facilitate the second cracking of light olefins that were already formed. With respect to the olefins distribution, light olefins derived from the bio-oil are dominated by ethylene and propylene together with a small amount of butylenes. The ethylene yield increased with increasing temperature. But the yields of propylene and butylenes decreased at high temperature, which is attributed to the secondary decomposition of these products.

C. Effect of S/C ratio

Figure 2 shows the effect of S/C ratio on the production of light olefins from the bio-oil over the HZSM-5 catalyst under the following conditions: T=600 °C, S/C=4−20 and WHSV=0.4 h^{-1}. With the increase of S/C from 4 to 10, the bio-oil conversion slightly increased. The olefins yield followed a similar trend as the bio-oil conversion. The butylenes distribution in the olefins product obviously ascended in the case of high S/C. Water is not a key reactant in the bio-oil catalytic pyrolysis. However, it can be used for adjusting the concentration of bio-oil in the catalyst bed and affect the bio-oil conversion process.

DOI:10.1088/1674-0068/25/04/441-447

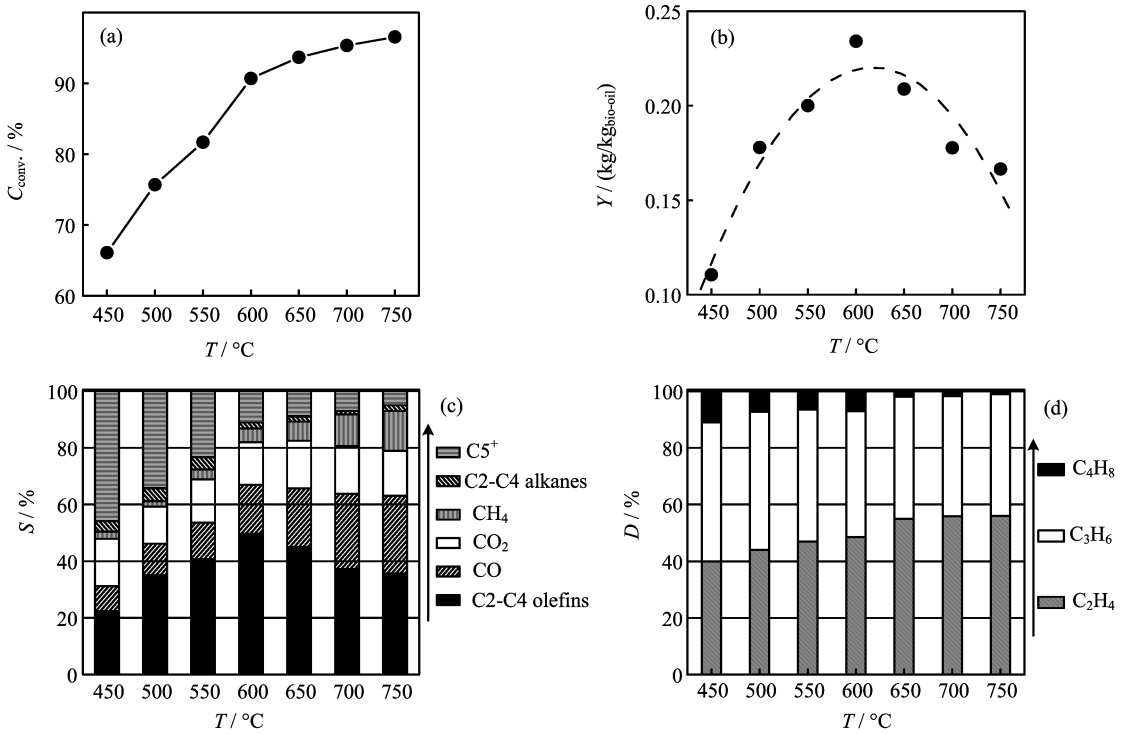

FIG. 1 Effect of temperature on the catalytic cracking of bio-oil over the HZSM-5 catalyst. (a) Carbon conversion, (b) yield of C2$^=$−C4$^=$ olefins, (c) selectivity of carbon-containing products, and (d) distribution of olefins. Reaction conditions: S/C=10, WHSV=0.4 h^{-1}.

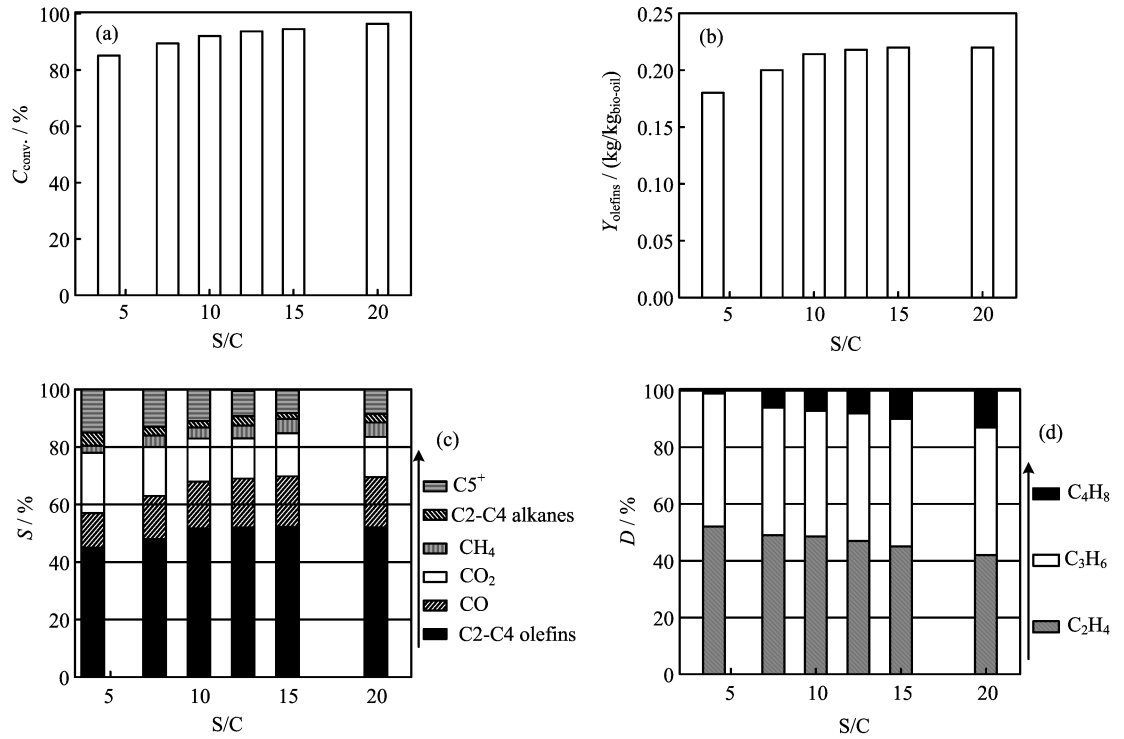

FIG. 2 Effect of S/C ratio on the catalytic cracking of bio-oil over the HZSM-5 catalyst. (a) Carbon conversion, (b) yield of C2$^=$−C4$^=$ olefins, (c) selectivity of carbon-containing products, and (d) distribution of olefins. Reaction conditions: T=600 °C, WHSV=0.4 h^{-1}.

DOI:10.1088/1674-0068/25/04/441-447

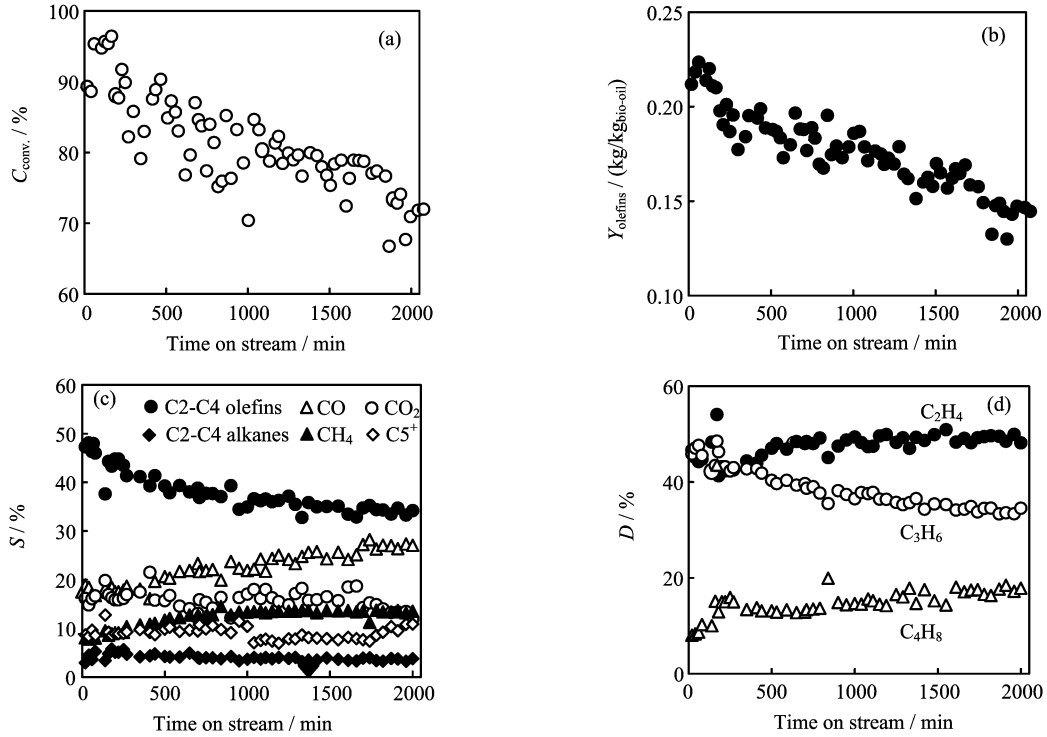

FIG. 3 Stability of catalyst during the catalytic cracking of bio-oil over HZSM-5 catalyst. (a) Carbon conversion, (b) yield of $C2^{=}-C4^{=}$ olefins, (c) distribution of olefins, and (d) selectivity of carbon-containing products. Reaction conditions: T=600 °C, S/C=10, WHSV=0.4 h^{-1}.

D. Catalyst stability in the catalytic pyrolysis of bio-oil

As shown in Fig.3, the catalyst stability in the catalytic pyrolysis of bio-oil was tested as a function of the time on stream under the optimized reaction conditions (T=600 °C, S/C=10, WHSV=0.4 h^{-1}). A slow decrease in the bio-oil conversion and olefins yield over the HZSM-5 catalyst were observed in 30 h period. The bio-oil conversion declined from the initial value about 95% to 70%. The yield of light olefins gradually decreased from 0.22 kg/kg$_{bio-oil}$ to 0.15 kg/kg$_{bio-oil}$. The selectivity towards light olefins slightly decreased, indicating that the impact of thermal pyrolysis was enhanced over the used catalyst. The decrease in the catalyst activity (*i.e.*, catalyst deactivation) is mainly attributed to the carbon deposition on the catalysts in the cracking of bio-oil as well as change in the property of the catalysts according to the following catalyst characterization.

E. Characterization of catalysts

The selected catalysts were characterized by means of XRD, NH_3-TPD, ^{29}Si MAS NMR, and TGA. Figure 4 shows the XRD spectra for the fresh and used catalysts of HZSM-5 after the bio-oil catalytic pyrolysis. For all the samples, the characteristic diffraction peaks at 8.0°, 8.8°, and 23.0° were clearly observed, which can be assigned to the crystal structure of ZSM-5 [27]. Meanwhile, a weak peak at around 45.2° was also identified and assigned to γ-Al_2O_3 phase. On the other hand, the decrease in the crystallinity of the zeolite catalysts was observed after the catalytic pyrolysis of bio-oil for 30 h, indicating that the framework structure was somewhat destroyed under the long-term hydrothermal condition.

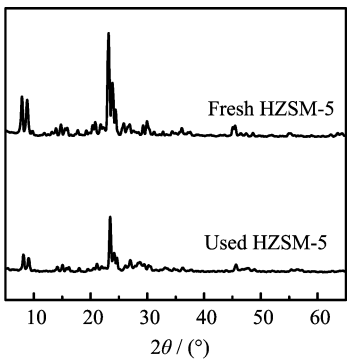

FIG. 4 XRD spectra for the fresh HZSM-5 and the used HZSM-5 catalysts after catalytic conversion of bio-oil for 30 h at T=600 °C, S/C=10, and WHSV=0.4 h^{-1}.

Figure 5 presents the NH_3-TPD profiles for HZSM-5 and the used catalyst after the bio-oil catalytic pyrolysis. All tested catalysts showed three acid sites with different acid strength. One strong peak around 220 °C was assigned to the desorption of NH_3 from the weak

DOI:10.1088/1674-0068/25/04/441-447

TABLE II Comparison between pyrolysis and catalytic pyrolysis of bio-oil with HZSM-5 catalyst at T=600 °C, S/C=10, WHSV=0.4 h^{-1}.

Catalysts	C/%	$Y_{olefins}$/(kg/$kg_{bio\text{-}oil}$)	S_X/%						D_n/%		
			$C2^=-C4^=$	CO	CO_2	CH_4	C2−C4	$C5^+$	C_2H_4	C_3H_6	C_4H_8
Pyrolysis	36.2	0.03	7.9	9.6	8.7	5.2	3.2	65.4	42.2	30.1	27.7
Catalytic pyrolysis	90.2	0.22	50.7	16.2	14.8	4.1	2.9	11.3	48.6	44.3	7.1

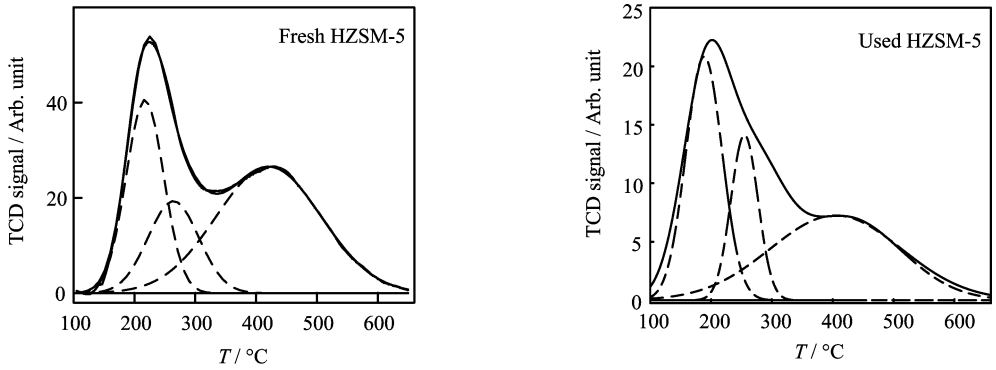

FIG. 5 NH_3-TPD spectra for the fresh HZSM-5 and used HZSM-5 catalysts after the catalytic conversion of bio-oil for 30 h at S/C=10 and WHSV=0.4 h^{-1}.

acid sites. Another profile of NH_3-TPD around 430 °C corresponded to the desorption of NH_3 from the strong acid sites [28]. The intersection between the strong and weak acid sites can be deconvolved into another Gaussian component, referring to NH_3 desorption from the medium acid sites (around 260 °C). With the analysis of the NH_3 desorption spectra, the total acid sites of the used catalysts obviously decreased from 580 μmol/g_{catal} to 231 μmol/g_{catal}. For fresh catalyst, the percentage of the strong acid, medium acid and weak acid sites was about 30:20:50, and changed to 35:18:47 for the used catalyst.

The ^{29}Si MAS NMR analysis was employed to investigate the Si-O-Al tetrahedral structure in the zeolite framework (Fig.6). For the original HZSM-5 catalyst, there was a strong peak near −112.5 ppm together with a shoulder at −115.8 ppm, which can be assigned to the Si (4 Si) species [28]. The profile in the low chemical-shift region (near −106.8 ppm) corresponded to Si (3 Si, 1 Al) sites (*i.e.*, Si atoms with one neighboring Al atom). The characteristic peaks of ^{29}Si MAS NMR from the used HZSM-5 catalyst were almost identical to that from the original HZSM-5, but the resonance peaks in the low chemical-shift region (−106.7 ppm) remarkably declined for the used ones. In addition, the framework silicon to aluminum ratio (Si/Al) could be estimated by the simulations of the ^{29}Si NMR spectra [28]. The Si/Al ratios for the fresh and used catalysts were about 25 and 48 respectively, suggesting that the zeolite suffered somewhat dealumination process under the hydrothermal condition. In addition, the rate of the carbon deposition on the TGA analysis was about 3.8 mg/(g_{catal}·h). Generally, the coke deposition will block the active sites and the pore channels of the catalyst, resulting in a decrease in the catalytic activity.

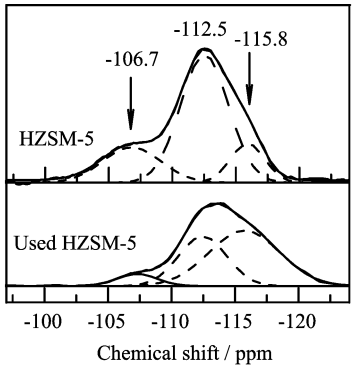

FIG. 6 ^{29}Si MAS NMR spectra for the fresh HZSM-5 and the used HZSM-5 catalysts after the catalytic conversion of bio-oil for 30 h at T=600 °C, S/C=10 and WHSV=0.4 h^{-1}.

F. Comparison between pyrolysis and catalytic pyrolysis of bio-oil

To further illustrate the transform of bio-oil into light olefins, the pyrolysis of bio-oil was separately investigated without catalyst. As shown in Table II, the products selectivity for the bio-oil pyrolysis is quite different from that for the catalytic pyrolysis of bio-oil. Main carbon-containing products observed in the high pyrolysis of bio-oil lined up as follows: $C5^+$ hydrocarbons>CO>CO_2>gaseous alkanes (mainly CH_4)>C2−C4 olefins. In addition, the yield

DOI:10.1088/1674-0068/25/04/441-447

of light olefins from the pyrolysis of bio-oil is less than 0.03 $kg/kg_{bio\text{-}oil}$ under our investigated conditions, which is much lower than the level from the catalytic cracking of bio-oil. The above results suggest that the pyrolysis of bio-oil is dominated by the decomposition of the heavier compounds towards lighter ones and gasification to mainly form CO, CO_2, and gaseous alkanes.

IV. CONCLUSION

Catalytic pyrolysis of bio-oil for the production of light olefins was performed by a series of molecular sieve catalysts. The highest olefins yield from bio-oil reached 0.22 $kg/kg_{bio\text{-}oil}$ with a selectivity of 50.7% and a nearly complete bio-oil conversion. The reaction parameters and the types of molecular sieve catalysts have an important impact on both olefins yield and its selectivity. The yield of light olefins from the pyrolysis of bio-oil is much lower than the level from the catalytic pyrolysis of bio-oil, and it is dominated by the decomposition of the heavier compounds towards lighter ones. The oxygenates in bio-oil may diffuse into the zeolite catalyst pores and undergo a series of reactions, mainly including decarbonylation, decarboxylation and dehydration to form olefins and other by-products. The conversion of bio-oil to light olefins may potentially provide a promising route for the production of the key petrochemical-light olefins using renewable biomass.

V. ACKNOWLEDGEMENTS

This work was supported by the National Natural Science Foundation of China (No.51161140331) and the National High Technology Research and Development of Ministry of Science and Technology of China (No.2009AA05Z435).

[1] N. Rahimi and R. Karimzadeh, Appl. Catal. A **398**, 1 (2011).
[2] Y. K. Park, C. W. Lee, N. Y. Kang, W. C. Choi, S. Choi, S. H. Oh, and D. S. Park, Catal. Surv. Asia **14**, 75 (2010).
[3] A. Corma, S. Iborra, and A. Velty, Chem. Rev. **107**, 2411 (2007).
[4] D. Bradin, Patent No.WO2008147836-A1, USA (2009).
[5] J. Cheng, P. Hu, P. Ellis, S. French, G. Kelly, and C. M. Lok, J. Catal. **257**, 221 (2008).
[6] M. M. Wright, D. E. Daugaard, J. A. Satrio, and R. C. Brown, Fuel **89**, 2 (2010).
[7] S. Czernik and A. V. Bridgwater, Energy Fuels **18**, 590 (2004).
[8] G. W. Huber and A. Corma, Angew. Chem. Int. Ed. **46**, 7184 (2007).
[9] S. Sun, H. Tian, Y. Zhao, R. Sun, and H. Zhou, Bioresour. Technol. **101**, 3678 (2010).
[10] A. G. Gayubo, A. T. Aguayo, A. Atutxa, R. Aguado, and J. Bilbao, Ind. Eng. Chem. Res. **43**, 2610 (2004).
[11] A. G. Gayubo, A. T. Aguayo, A. Atutxa, R. Aguado, M. Olazar, and J. Bilbao, Ind. Eng. Chem. Res. **43**, 2619 (2004).
[12] A. G. Gayubo, B. Valle, A. T. Aguayo, M. Olazar, and J. Bilbao, Ind. Eng. Chem. Res. **49**, 123 (2010).
[13] T. P. Vispute, H. Y. Zhang, A. Sanna, R. Xiao, and G. W. Huber, Science **330**, 1222 (2010)
[14] P. Gallezot, ChemSus Chem. **1**, 734 (2008).
[15] A. Corma, M. J. Diaz-Cabanas, J. Martinez-Triguero, F. Rey, and J. A. Rius, Nature **418**, 514 (2002).
[16] C. Marcilly, J. Catal. **216**, 47 (2003).
[17] S. Czernik and A. V. Bridgwater, Energy Fuels **18**, 590 (2004).
[18] A. Corma, G. W. Huber, L. Sauvanaud, and P. O'Connor, J. Catal. **247**, 307 (2007).
[19] M. Stöcker, Angew Chem. Int. Ed. **47**, 9200 (2008).
[20] J. J. Bozell, Science **329**, 522 (2010).
[21] F. Y. Gong, T. Q. Ye, L. X. Yuan, T. Kan, Y. Torimoto, M. Yamamoto, and Q. X. Li, Green Chem. **11**, 2001 (2009).
[22] L. X. Yuan, Y. Q. Chen, C. F. Song, T. Q. Ye, Q. X. Guo, Q. S. Zhu, Y. Torimoto, and Q. X. Li, Chem. Commun. 5215 (2008).
[23] T. Hou, L. X. Yuan, T. Q. Ye, L. Gong, J. Tu, M. Yamamoto, Y. Torimoto, and Q. X. Li, Int. J. Hydrogen Energy **34**, 9095 (2009).
[24] T. Kan, J. X. Xiong, X. L. Li, T. Q. Ye, L. X. Yuan, Y. Torimoto, M. Yamamoto, and Q. X. Li, Int. J. Hydrogen Energy **35**, 518 (2010).
[25] Y. Xu, T. Q. Ye, S. B. Qiu, S. Ning, F. Y. Gong, Y. Liu, and Q. X. Li, Bioresour. Technol. **102**, 6239 (2011).
[26] D. S. Zhang, R. J. Wang, and X. X. Yang, Micropor. Mesopor. Mat. **126**, 8 (2009).
[27] X. J. Li, S. L. Liu, X. X. Zhu, Y. Z. Wang, S. J. Xie, W. J. Xin, L. Zhang, and L. Y. Xu, Catal. Lett. **141**, 1498 (2011).
[28] F. Y. Gong, Z. Yang, C. G. Hong, W. W. Huang, S. Ning, Z. X. Zhang, Y. Xu, and Q. X. Li, Bioresour. Technol. **102**, 9247 (2011).

DOI:10.1088/1674-0068/25/04/441-447